

Article

Framework for Assessing Impact of Wave-Powered Desalination on Resilience of Coastal Communities

Kelley Ruehl ^{1,*} , Katherine A. Klise ¹ , Megan Hinks ²  and Jeff Grasberger ¹ ¹ Energy Water Systems Integration Department, Sandia National Laboratories, Albuquerque, NM 87185, USA; kaklise@sandia.gov (K.A.K.); jtgrasb@sandia.gov (J.G.)² Department of Ocean Engineering, Texas A&M University, College Station, TX 77843, USA; meganhinks@tamu.edu

* Correspondence: kelly.ruehl@sandia.gov

Abstract: Coastal communities face unique challenges in maintaining continuous service from critical infrastructure. This research advances capabilities for evaluating the impact of using wave energy to desalinate water on the resilience of coastal communities. The study focuses on the feasibility of using wave energy conversion to provide drinking water to communities in need and applying resilience metrics to quantify its impact on the community. To assess the feasibility of wave-powered desalination, this research couples the open-source software Wave Energy Converter Simulator (WEC-Sim) and Water Network Tool for Resilience (WNTR). This research explores variations in both the wave resource (location, seasonality, and duration) and the ability to maintain drinking water service during a disruption scenario by applying the simulation framework to three case studies, which are based on communities in Puerto Rico. The simulation framework provides a contextualized assessment of the ability of wave-powered desalination to improve the resilience of coastal communities, which can serve as a methodology for future studies seeking the integration of wave-powered desalination with water distribution systems.

Keywords: wave energy; water distribution systems; desalination; remote coastal communities; WEC-Sim; WNTR



Academic Editors: Pedro Cabrera and Enrique Rosales Asensio

Received: 19 December 2024

Revised: 9 January 2025

Accepted: 11 January 2025

Published: 24 January 2025

Citation: Ruehl, K.; Klise, K.A.; Hinks, M.; Grasberger, J. Framework for Assessing Impact of Wave-Powered Desalination on Resilience of Coastal Communities. *J. Mar. Sci. Eng.* **2025**, *13*, 219. <https://doi.org/10.3390/jmse13020219>

Copyright: © 2025 by the authors. Licensee MDPI, Basel, Switzerland. This article is an open access article distributed under the terms and conditions of the Creative Commons Attribution (CC BY) license (<https://creativecommons.org/licenses/by/4.0/>).

1. Introduction

In 2019, the Department of Energy (DOE) Water Power Technologies Office launched the Powering the Blue Economy (PBE) initiative, outlining applications for marine energy to serve human needs, mitigate climate change, and stimulate economic growth [1]. Wave energy emerged as a promising method in achieving PBE goals, as well as meeting the pledge of carbon neutrality by 2050 [2]. Compared to other renewable sources, wave energy converters (WECs) are operable 90% of the time, whereas wind and solar systems produce power 20 to 30% of the time [3]. However, wave energy is an emerging field with high capital costs and levelized cost of energy, thus making wave energy projects economically challenging. In alignment with PBE goals, using wave energy to desalinate water has been explored as a potential application with economic viability. The costs of wave energy conversion can vary significantly based on location, type, and components in terms of the installation, operations, and maintenance costs [4], but the ability to produce water directly without conversion to electricity can be economically advantageous. Wave-powered desalination can potentially reduce the cost of water as the levelized cost of water of desalinated water is comparable to market prices [5].

Infrastructure for water distribution and electricity production are critical for daily life, but coastal communities, and especially remote island communities, often face scarcity of both. Furthermore, energy and water are fundamentally interconnected. Power is required to run pumps that distribute water throughout communities, and likewise, water is often required to produce electricity [6]. In addition, as technology and economies advance, electricity demands increase concurrently. This puts added strain on already limited water supplies to meet the demand [7]. Reverse Osmosis (RO) desalination is more energy efficient than traditional thermal desalination systems and is, therefore, used more commonly [8]. However, RO desalination requires pressure to feed saltwater through the RO membranes, often requiring a large amount of energy. In prior research, Yu and Jenne [8] demonstrated that wave energy has the ability to generate sufficient pressure to run an RO system and generate freshwater permeate, without the need for electrical power. This is especially interesting from a resilience point of view because it largely decouples water distribution and electricity production.

According to the National Oceanic and Atmospheric Administration, about 40 percent of the global population resides in coastal counties [9], and wave energy provides a renewable resource that is collocated with population centers. This is beneficial for islands with limited space and proximity to high-density wave fields. Due to its collocation, efficiency losses from transmitting energy and water across long distances can also be minimized. One of the main goals for the PBE initiative is to improve access and increase the resilience of energy resources and clean water for remote coastal communities [1]. Island communities face limited electrical grid connection and water scarcity and often rely on imported fossil fuels to meet their needs, thus causing the cost of water and electricity to be higher. Additionally, their susceptibility to natural disasters and geographic isolation increases the need for robust and resilient infrastructure. Furthermore, climate change poses a large risk to these communities as sea level rise, droughts, and flooding impact the already limited water supplies [10,11].

The objective of this paper is to establish a framework for evaluating the impact of wave-powered desalination on the ability to provide drinking water to coastal communities. The following sections describe the simulation framework and the results of applying it to three case studies, which are based on communities in Puerto Rico.

2. Simulation Framework

The feasibility of using wave energy to desalinate water and provide water to communities was assessed by coupling the Wave Energy Converter SIMulator (WEC-Sim) [12,13] and the Water Network Tool for Resilience (WNTR) [14]. This simulation framework was used to explore scenarios that varied the size of the wave farm, its location, and seasonality. The simulations assume existing power generation is readily available, but water supplies are limited, and a wave-powered desalination plant is used to deliver water to the community.

The feasibility study evaluated a desalination plant powered by wave farms of one to five WECs. WEC-Sim was used to simulate the dynamics and performance of the wave energy converter(s) and included a model of the RO desalination plant, building upon prior work by Yu and Jenne [8]. WNTR was used to simulate the hydraulics of the water distribution system, which can include disaster scenarios that affect supply, demand, and component failure. WNTR has analyzed the resilience of drinking water utilities across the U.S., including earthquake resilience in California [14], hurricane resilience in the U.S. Virgin Islands [15], source water vulnerability in New York [16], and water service disruptions at several military installations. The results of the analysis help prioritize investments that reduce water service disruptions. In this analysis, metrics were also

defined to evaluate the impact of wave-powered desalination on the resilience of coastal communities. These resilience metrics are used to assess how wave-powered desalination affects response to disaster scenarios, like disruption of service due to natural disasters (e.g., hurricanes). Survival of WECs to extreme events is a challenge that has garnered a lot of attention from WEC developers with various analysis methods and survival strategies [17]. The WECs proposed here could be designed to survive necessary conditions or designed to be deployed following the event. This simulation framework was then applied to communities in Puerto Rico as a case study due to the importance of restoring services to Puerto Rico after a natural disaster, but the modeling approach can be applied to other locations in the future. The following sections describe the methods used in developing the coupled WEC-Sim and WNTR framework.

2.1. Wave-Powered Desalination Plant

WEC-Sim was used in this study to model the wave-powered desalination plant. In WEC-Sim, WECs are simulated by specifying the device geometry, joints and constraints, power take-off system components, and mooring system, and they can also include control algorithms. WEC-Sim models are often used to simulate device performance and can be used to improve upon existing designs.

A single WEC wave-powered desalination plant, consisting of an oscillating surge wave energy converter (OSWEC) coupled with an RO desalination plant, was originally developed and validated by Yu and Jenne in 2018 [8]. Yu and Jenne's OSWEC RO model was developed for the six Wave Energy Prize operational sea states, which are much more energetic than the available resources in Puerto Rico [18]. Prior to applying the OSWEC model to the Puerto Rico wave resource, the authors confirmed that they were able to reproduce the results previously validated by Yu and Jenne [8]. The model was then rerun using a wave resource based on the Puerto Rico wave environment. The results were that the single OSWEC RO model produced significantly less water for the Puerto Rico wave resource. To produce a comparable amount of water in Puerto Rico, the number of OSWEC devices was increased, and wave farms of one to five WECs were evaluated. The boundary element method (BEM) solver WAMIT [19] was used to calculate the hydrodynamic coefficients for each of the wave farm configurations, a necessary pre-processing step for WEC-Sim. WEC-Sim models were then developed for wave farms consisting of one to five OSWECs, each of which included the RO desalination plant model. Figure 1 shows the WEC-Sim model of the wave-powered desalination plant for a wave farm of five WECs.

First, each wave farm configuration was run for a 1 h simulation using a Pierson–Moskowitz spectrum with a significant wave height (H_s) of 0.75 m and peak period (T_p) of 5 s [18], waves representative of the Puerto Rico wave resource. These 1 h simulations were used to ensure the WEC-Sim models were stable and to provide a preliminary estimate of the amount of desalinated water, i.e., permeate, produced for each wave farm configuration. For reference, the 1 h simulation of the single WEC took about twenty minutes to run (faster than real-time), whereas the 1 h simulation of five WECs took about sixty minutes to run (about real time) on a standard PC. The results from these preliminary 1 h simulations are shown in Table 1.

These 1 h simulations were an important first step to establish the stability of the baseline wave-powered desalination plant model in WEC-Sim. Since they could be run relatively quickly, they were also used to establish the simulation framework and develop resilience metrics. Each of the wave farm configurations was then run for a 24 h simulation using wave data measured by the National Data Buoy Center (NDBC) [20]. The WEC-Sim models for each of the wave farm configurations were run using 24 h of wave data to simulate a full day. The 24 h simulation of the single WEC took about eight hours to

run, whereas the 24 h simulation of five WECs took about 24 h to run. The permeate from WEC-Sim for each hour was then used as the input for the WNTR water distribution system model, as described below. Due to the computation cost of running these 24 h simulations, Sandia's high-performance computing (HPC) resources were used for the WEC-Sim runs to reduce the runtime.

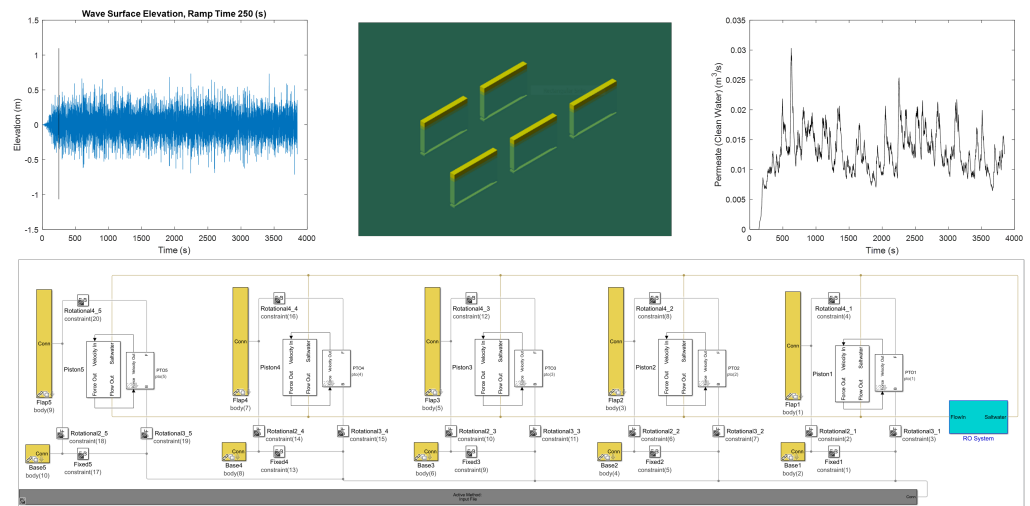


Figure 1. WEC-Sim model of a wave-powered desalination plant for the five OSWEC farms: (Top Left) Wave resource; (Top Middle) WEC-Sim visualization; (Top Right) Produced water; (Bottom) WEC-Sim model of five WEC farms with an RO desalination plant.

Table 1. Summary of WEC-Sim results for 1 h simulations using a Pierson–Moskowitz spectrum with $H_s = 0.75$ m and $T_p = 5$ s.

WEC Farm	1 WEC	2 WEC	3 WEC	4 WEC	5 WEC
Average permeate (m ³ /s)	0.0013	0.0066	0.0087	0.0112	0.0133

2.2. Water Distribution System

Drinking water utilities commonly use simulation and analysis tools to better understand system hydraulics and water quality under a range of normal and abnormal conditions. A typical numerical model of a water distribution system includes the pipe layout and characteristics, pump and valve operations, storage tanks, consumer demand, and clean water supplied from water treatment facilities. The model allows the utility to test out new modes of operations, which may provide improved performance under various circumstances. In this study, WNTR was used to model the water distribution system operated with the integration of desalinated water from a WEC farm.

The water distribution system model used in the simulation framework is based on a simplified version of the Guayama, Puerto Rico water distribution system, shown in Figure 2. This simplified model includes 16 junctions and represents the water system demands and basic structural layout. This information was obtained from open-source infrastructure data [21] and through collaboration with the Puerto Rico Aqueduct and Sewer Authority (PRASA). It is assumed that the water distribution system serves 40,000 people and that the water consumption rate is 100 gallons per person per day. This results in 4 million gallons per day (approximately 15,000 m³/day or 0.17 m³/s). Under normal operating conditions, the main water treatment facility in Guayama can produce and distribute water needs across the city.

This analysis considers a disruption scenario where the water treatment facility is compromised, and the utility could pull water from a secondary desalination water treatment

plant that is located along the coast, i.e., the wave-powered desalination plant. The disruption limits flow from the existing water treatment plant to 50% of normal operation. The disruption is simulated over a 14 day duration. All WNTR simulations use pressure-dependent simulation, with a required pressure of 21.1 m (30 psi) to meet the expected demand.

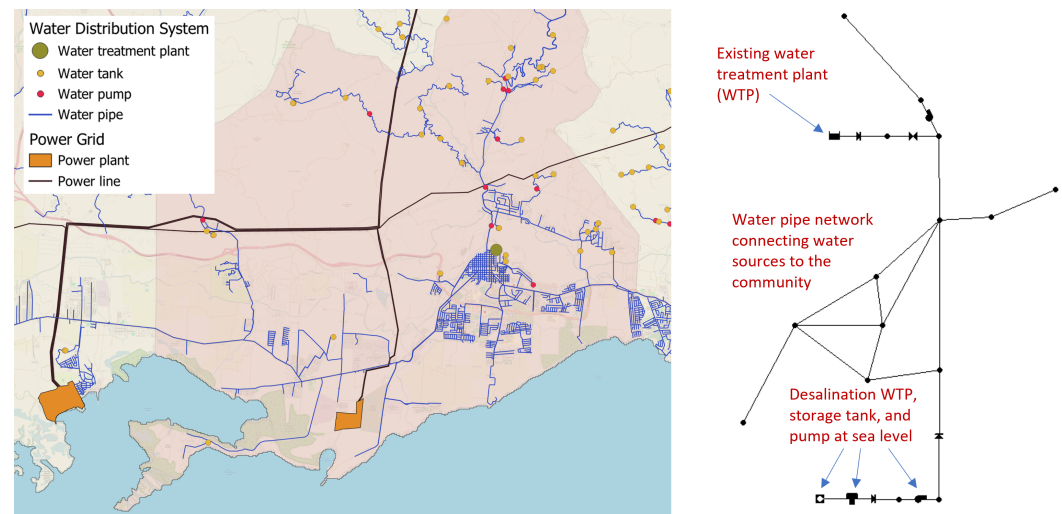


Figure 2. (Left) Guayama water distribution system and power grid data (Right) Simplified water distribution system model with a main water treatment facility and secondary desalination facility, storage, and pump.

The desalination plant is modeled in WNTR, using several components, including the following: (1) A desalination water source, which uses the permeate production rate from WEC-Sim; (2) A tank, which can store desalinated water that is not needed at the time of production; (3) A pump to move desalinated water from sea level to customers. Currently, because the water distribution model is run on an hourly time-step, the average hourly permeate from WEC-Sim is used to model desalination water production. The hourly permeate results from WEC-Sim are stored in a text file, which are used in the WNTR simulations. The storage tank can hold up to 1 million gallons of water (approximately 3800 m³). This is equivalent to 25% of the daily water needs in Guayama. The pump at the desalination plant has the capacity to pump 10% of the total community water needs (0.017 m³/s in Guayama) to an elevation of 125 ft (38.1 m). This elevation is sufficient to reach consumers that reside at elevations well below the traditional water treatment facility (which resides at 360 ft above sea level). Power requirements for this pump are approximately 6.5 kW. The power requirements for pumping across the rest of the water distribution system are around 77 kW. These values assume a pump efficiency of 70%. Under conditions where flow from the main water treatment plant is compromised, water from the storage tank at the desalination plant can be pumped to supplement community water needs. The WNTR simulations for this analysis run on a standard PC in a few minutes. Analysis that includes a more detailed numerical model, shorter hydraulic time steps, and additional scenarios can increase runtime significantly. For those cases, WNTR can be run on HPC resources to reduce runtime.

2.3. Resilience Metrics

The coupled WEC-Sim and WNTR model of the wave-powered desalination plant and water distribution system described above were used to run coupled analyses with varying wave conditions and wave farm configurations. Results from the coupled analysis were translated into resilience metrics that quantify the impact of wave-powered desalination on the resilience of coastal communities. Each of these metrics provides insight into the benefit

of wave-powered desalination on the community's resilience. These resilience metrics were based on results from WEC-Sim and WNTR. The resilience metrics from WEC-Sim were based on prior work from Yu and Jenne, while those from WNTR are standard outputs from WNTR [8,22]. A description of how each metric relates to community resilience is defined in Table 2.

Table 2. Wave-powered desalination resilience metrics.

Resilience Metric	Description
Average permeate (m ³ /s)	Average volume of water produced by the desalination plant
Water demand (%)	Percent of community water needs produced by the desalination plant
Average pressure (m)	Average pressure in the water distribution system during the disruption
Average WSA (%)	Average water service availability (WSA), which is defined as the percentage of community's expected water needs that are met during the disruption
Pump power (kW)	Power required to pump water produced by the desalination plant during the disruption

These resilience metrics can be used to better understand the impact of wave-powered desalination on resilience to disruption of water service due to natural disasters (e.g., hurricanes). While these metrics are reported as singular values or system averages, the percent of permeate received and water service availability (WSA) can also be reported per water network junction. Average permeate and water demand are determined based on WEC-Sim outputs. Average permeate is the volume of water made available to the community exclusively from wave-powered desalination, and the water demand is the percentage of water made available to the community based on the community's population and water consumption rate. For water demand, the water consumption rate is assumed to be 100 gallons/person/day. WNTR provides the resilience metrics for average water distribution system pressure, WSA, and pump power. In the case of average water distribution system pressure, adequate water pressure is required to meet community water needs, including drinking water, industrial water use, and firefighting. The average WSA is defined as the ratio of delivered demand to the expected demand. Pump power, as detailed in the water distribution system section above, is the power necessary to transport water through the distribution system and to the community. These metrics are computed using the disruption scenario where water supplies are limited from the existing water treatment plant.

3. Puerto Rico

Puerto Rico was chosen as the site of interest for this feasibility study. Puerto Rico is home to about 3.3 million residents, with its largest population density concentrated in the northern part of the island in San Juan, Bayamon, and Carolina [23]. The main sources of water in Puerto Rico are surface water and groundwater [24]. Moreover, 70% of the total groundwater contribution is withdrawn from the North Coast Limestone aquifer system and the South Coastal Alluvial Plain aquifer system, both of which have shown evidence of overdraft [25]. This occurs when water is being withdrawn from aquifers at a faster rate than it is being replenished. In addition, these aquifers are connected to the ocean, and as water levels inside the reservoirs fall or if the sea level rises, there is an increased risk of saltwater infiltrating the wells [26].

Aquifers are recharged by rainfall or surface water sources, both of which are susceptible to climate change. Droughts are a huge threat to aquifer restoration, as frequent dry seasons cause the water level to lower each year. The severity and duration of droughts are intensified by climate change [27]. As a consequence of years of below-average rainfall, one of the most extreme droughts in Puerto Rico occurred in 2015. Millions of people faced water insecurity and suffered from the strictest water rationing in the history of Puerto Rico [28]. The impacts of the drought were exacerbated by water levels in the South Coastal Alluvial Plain aquifer system progressively declining over the past 20 years. Following the extreme drought, the volume of groundwater had dropped to the lowest recorded level at 31 feet below the surface. This was detrimental to the community and environment of Salinas, which relied exclusively on the aquifer for water [29].

Puerto Rico is also susceptible to hurricanes, which have intensified due to climate change [30]. Two years after the 2015 drought, Hurricane Maria made landfall in Puerto Rico as a Category 4 storm and decimated the island. Five years later, Hurricane Fiona further damaged the systems that had never fully recovered from Maria [31]. The damage to the electric grid caused major disruptions in water service and blackouts across the island, leaving some residents without electricity for close to a year [28].

Puerto Rico consumes more energy than it produces and relies on imported petroleum products to meet its energy demand [32]. Because of a lack of energy diversification, poor maintenance on the system, absence of necessary modernization, and natural disasters, Puerto Rico passed the Puerto Rico Energy Public Policy Act (PREPPA) in 2019 to codify the specifications for a reliable, resilient, and affordable energy system [31]. In addition, Puerto Rico codified goals to completely phase out coal-fired energy production by 2028 with interim milestones, such as an energy system composed of 40% renewable sources by 2025 and 60% by 2040, with a call for 30% increase in energy efficiency that same year [31]. PREPPA also sets the precedent that LUMA Energy, the electric power company of Puerto Rico, must obtain 100% of energy production from renewable sources by 2050 [31].

To lessen the burden on these resources, the diversification of water sources strengthens the resilience of these communities to the effects of climate change and natural disasters. Seawater desalination has been designated as the main water supply in neighboring islands such as St. Croix and St. Thomas [33]. Using wave energy to power a desalination plant not only meets the goals for PBE and PREPPA but also has the ability to produce the pressure required to push water through RO membranes, removing the need for additional power production to generate permeate and its resulting strain on the electric grid [8].

3.1. Case Studies

The simulation framework is applied to three case study locations across Puerto Rico: Guayama, San Juan, and Arecibo. The wave resource for each location is defined using National Data Buoy Center (NDBC) wave data from the nearest buoy: the Ponce Buoy (42085) for Guayama, San Juan Buoy (41053) for San Juan, and Arecibo Buoy (41121) for Arecibo [20]. The Guayama and San Juan case studies use NDBC data from 2020. However, data were not available for Arecibo (41121) in 2020, so 2022 data were used instead. While each community has a unique water distribution system, this analysis uses the same simplified Guayama water distribution network model for each case study. However, each case study scales drinking water demands using 2020 census population data [34]. The storage tank that can hold up to 1 million gallons of water from the desalination plant was not changed for each site. The three case study locations are listed in Table 3, and they use NDBC wave data and the most recent census information for population sizes.

Table 3. Case study locations, wave resource, population, and water consumption.

	Case 1—Guayama	Case 2—San Juan	Case 3—Arecibo
NDBC Buoy Year	Ponce (42085) 2020	San Juan (41053) 2020	Arecibo (41121) 2022
Mean significant wave height, H_s (m)	0.91	1.36	1.25
Mean peak wave period, T_p (s)	6.07	9.17	8.59
Population	40,000	342,000	90,000
Mean water consumption rate, m^3/s	0.17	1.50	0.39

3.2. Wave Resource

The wave resources for Guayama, San Juan, and Arecibo were assessed using historical data from 2020 and 2022, using the NDBC buoys listed in Table 3 [20]. Guayama is located on the south shore of Puerto Rico, whereas San Juan and Arecibo are located on the north shore. The south shore typically has a smaller wave resource than the north shore [18]. As a result, it is expected that the same wave farm will produce more permeate in San Juan and Arecibo than in Guayama. The variability of the wave resource for each location is shown in Figure 3. For example, in January 2022, the mean wave heights were 0.87 m, 1.30 m, and 1.27 m for Guayama, San Juan, and Puerto Rico, respectively. The corresponding wave periods are 5.76 s, 10.78 s, and 10.72 s, respectively. In January 2022, the north shore had larger wave heights and longer wave periods than the south shore, a trend that is also present in the January 2020 data. This is noteworthy because the Guayama and San Juan case studies were completed first using NDBC data from January 2020, and the Arecibo case study was added later. Unfortunately, Arecibo NDBC 41121 did not have data for January 2020, so the Arecibo case study was evaluated using data from 2022. While there is variability in the resource from 2020 to 2022, Figure 3 shows that the mean wave resource is similar. For example, Guayama's January mean wave height was 0.88 m in 2020 and 0.87 m in 2022, and its wave period was 6.24 s in 2020 and 5.76 s in 2022. San Juan's resource between 2020 and 2022 has more variability. San Juan's January mean wave height was 1.68 m in 2020 and 1.30 m in 2022, and its wave period was 10.1 s in 2020 and 10.8 s in 2022.

Figure 3 also compares the mean wave height and period for the entire month to the mean of the first day of that month. For example, Figure 3a shows the mean resource in Guayama for the month of January in 2020 and 2022, compared to the mean resource for 1 January of each year. The mean wave height and period of the first day of each month are included because each case study was evaluated for a 24 h period using NDBC data for the first day of that month. For Guayama and San Juan, this 24 h period is from 1 January 2022. For Arecibo, the 24 h period is from 1 January 2020.

Furthermore, the seasonality of the wave resource was explored for the Arecibo case study. The 24 h periods for this seasonality assessment correspond to NDBC data from 1 January, 1 April, 1 July, and 1 October in 2020. Figure 3c,d show the mean wave period and mean wave height for each month, compared to the first day of that same month. The largest monthly mean wave height is 1.43 m in April 2022, and the smallest is 0.91 m in October 2022. The mean monthly wave period also changes seasonally, with the longest at 10.7 s in January 2022 and the shortest at 6.56 s in October 2022. Since wave energy is

proportional to the square of wave height, it is expected for a wave farm located in Arecibo to produce more permeate in April than in October, based on data from 2022.

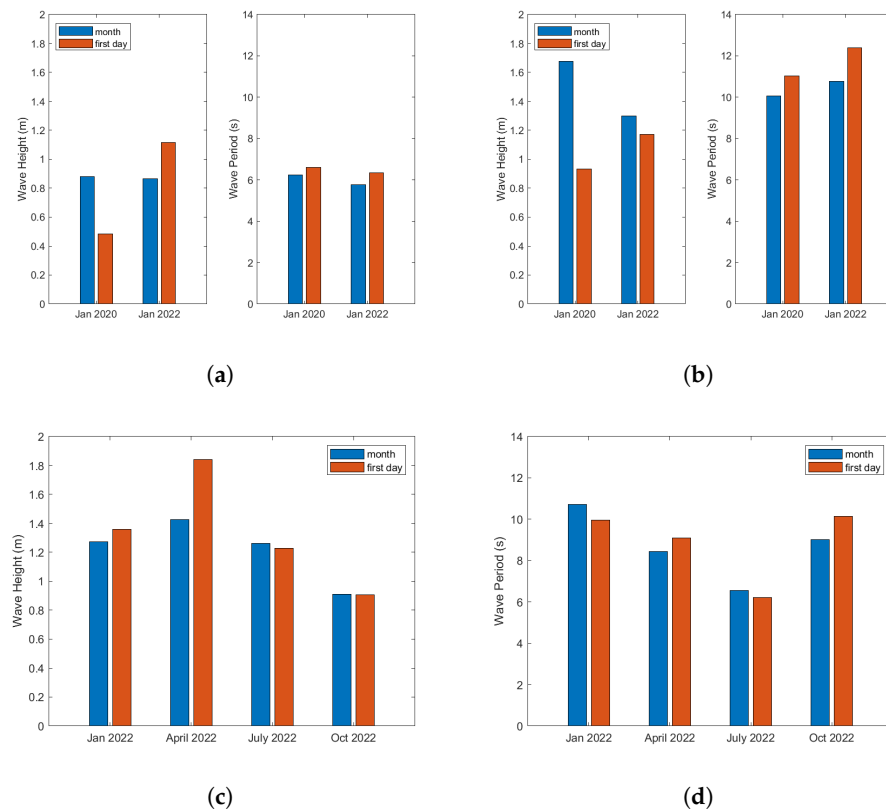


Figure 3. Wave resource for Guayama, San Juan, and Arecibo: (a) Guayama wave height and period. (b) San Juan wave height and period. (c) Arecibo wave height. (d) Arecibo wave period.

4. Results

This section discusses the case study results, which apply the simulation framework to three different communities in Puerto Rico: Guayama, San Juan, and Arecibo. For each location, normal operation of the water treatment plant provides the water distribution system with an average pressure of 60 m and an average WSA of >99%. To evaluate the benefit of an additional wave-powered desalination plant, the disruption scenario limits the existing WTP to 50% of its normal flow rate. WEC-Sim results are based on 24 h wave resource data from 1 January, and an additional seasonality analysis was run for Arecibo. WNTR results are based on a 14 day simulation using water demand scaled to each location's population.

4.1. Guayama Case Study

The community selected for the first case study is Guayama, located on the south shore of Puerto Rico. Guayama has a population of 40,000 and water use of 4 million gallons per day (approximately 15,000 m³/day or 0.17 m³/s). Since the original water distribution system model is based on Guayama, the model did not need to be re-scaled. The results from the 24 h simulation based on a full day of NDBC Ponce (42085) buoy data from 1 January 2020 are shown in Table 4. Figure 4 shows the time series of the 24 h permeate and 14 day WSA, based on simulation results. The results show that increasing the size of the wave farm has a substantial impact on the amount of permeate produced and its resulting WSA.

The WEC-Sim results in Table 4 show that a desalination plant powered by one WEC can produce 4.6% of the Guayama's daily water supply (i.e., water demand), two WECs can

produce about 10%, and five WECs can produce 18.4%. While the single WEC produces a decent volume of permeate, increasing the farm size substantially increases the volume of permeate, where the permeate production by the five WEC farms is limited by the capacity of the desalination plant. Due to the nonlinear nature of the system, the single WEC results could not be extrapolated to estimate the results of the larger arrays. Instead, each array configuration was run independently. The permeate and corresponding water demands more than double from the single WEC configuration to the two WEC farms. The permeate outputs start with 0.0079 m³/s for one WEC and increase to 0.0173 m³/s for two WECs. From there, the average permeate outputs steadily increase to 0.0312 m³/s for five WECs.

The WNTR results in Table 4 show that average pressure increases from 21.8 with 0 WECs to 27.1 m when all five WECs are used. Note that while the disruption scenario decreases flow from the existing water treatment to 50%, the average WSA is 52% even when no WECs are in use. This inconsistency is attributed to numerical error and fluctuations in WSA over time. WSA increases from 52% to 68%, closely matching the 18% increase in permeate water demand when all five WECs are in use. This means that all of the permeate water is being used to meet water needs of the community. While the overall WSA can be approximated from the WEC-Sim results, the spatial distribution of water service can vary significantly. For example, the community needs to ensure continuous water service at specific locations like hospitals. The pump power approaches 24 kW as the number of WECs increases from one to five. This is related to the amount of time the pumps are on. Higher rates of permeate fill the desalination tank faster, allowing the pump to pull water into the water distribution system at a constant rate.

Table 4. Summary of results for Guayama case study.

Software	Resilience Metric	Number of WECs					
		None	1	2	3	4	5
WEC-Sim	Average permeate (m ³ /s)	0	0.0079	0.0173	0.0232	0.0278	0.0312
	Water demand (%)	0.0%	4.6%	10.2%	13.6%	16.4%	18.4%
WNTR	Average pressure (m)	21.8	23.1	25.0	26.0	27.0	27.1
	Average WSA (%)	52%	56%	62%	64%	68%	68%
	Pump power (kW)	0.0	6.2	14.5	18.9	23.6	23.8

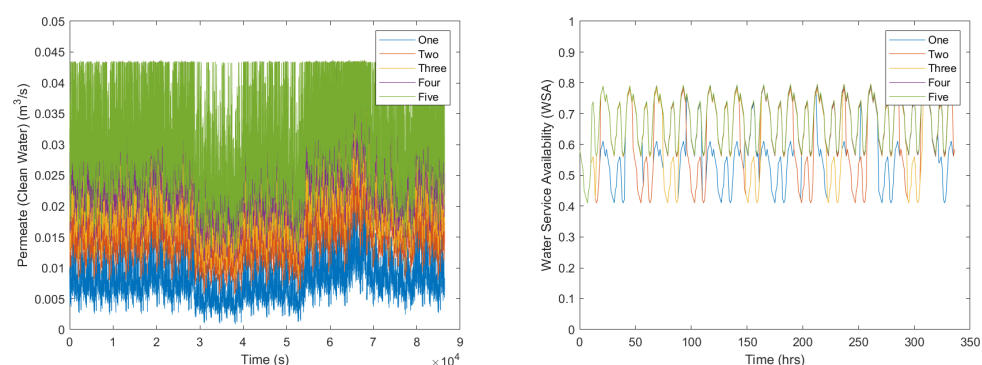


Figure 4. (Left) The 24 h time series of permeate from one to five WEC farms in Guayama. (Right) The 14 day time series of WSA, using the one to five WEC farms.

4.2. San Juan Case Study

Located on the north shore, which has a larger available wave resource, San Juan was evaluated for the second case study. It also has a much greater population than Guayama, and as a result, the water demand assumptions were scaled accordingly. The population of San Juan is about 342,000 and the water consumption rate is kept at 100 gallons per person per day [34]. As a result, the demand in San Juan is assumed to be 34.2 million gallons

per day (about $130,000 \text{ m}^3/\text{day}$ or $1.50 \text{ m}^3/\text{s}$), which is much higher than the demand in Guayama. The results from the 24 h simulation based on a full day of NDBC San Juan (41053) buoy data from 1 January 2020 are shown in Table 5. Figure 5 shows the time series of the wave surface elevation and permeate for the five WEC farms over the 24 h period, with each hour of analysis shown in a new color. These results show that the permeate produced by the wave-powered desalination plant for the five WEC farms is limited by the capacity of the desalination plant. To produce more permeate and not be capacity limited, the desalination plant would need to be resized for the San Juan resource.

The San Juan desalination plant produces more permeate due to its larger wave resource. The results follow a similar pattern as seen in the Guayama case study, where the average permeate and percent water demand met almost double between one WEC and two WEC arrays. For the five WEC farms, the average permeate is $0.0348 \text{ m}^3/\text{s}$, which corresponds to 2.3% of the community's water demand.

The sizeable increase in population between Guayama and San Juan has a significant impact on the percent of water demand that can be met with permeate. In Guayama, one WEC produced 4.6% of the community's water demand, compared to 0.9% by the same configuration in San Juan. This trend progresses through each of the wave array configurations, resulting in the five WEC arrays producing 18.4% of water demand in Guayama, compared to 2.3% in San Juan. While the average permeate output in the San Juan plant is greater, the percentage of water demand met is minimal due to the size of the population.

These results carry over to simulations of the water distribution system. The WNTR results show a minimal impact on water pressure and WSA. Low average water pressure indicates that the compromised system is not capable of providing high pressure water for firefighting. The pump power is similar to the Guayama case study, given the ability of the desalination plant to quickly fill the holding tank.

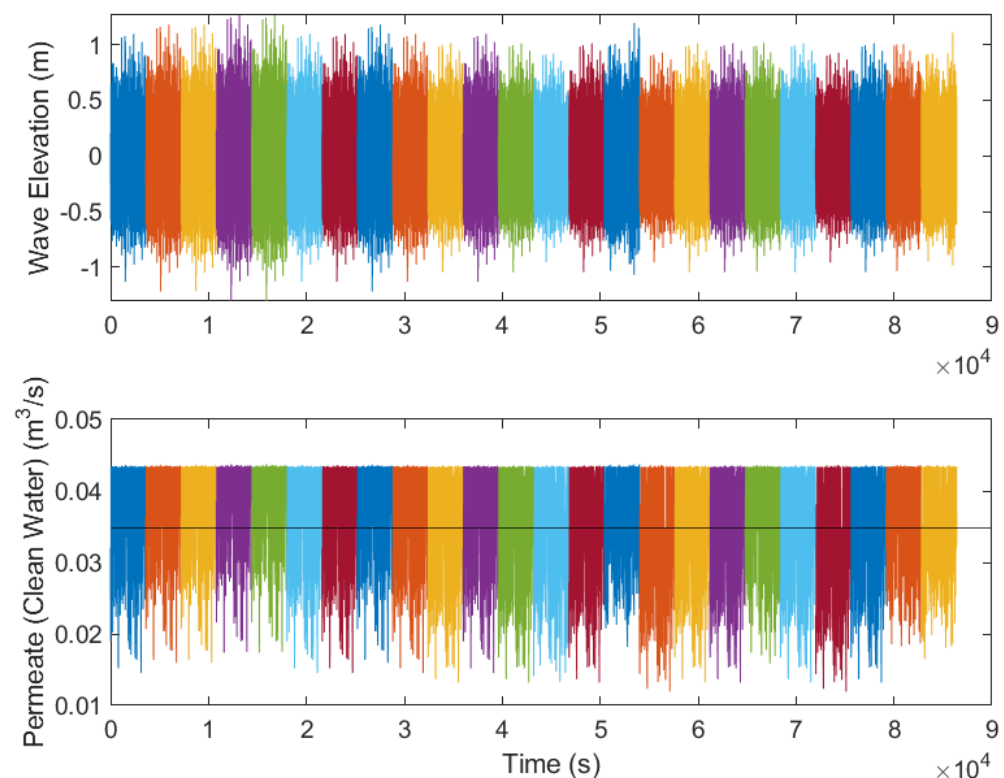


Figure 5. The 24 h results for the five San Juan WEC farms in January: **(Top)** Wave surface elevation from NDBC San Juan (41053) buoy data. **(Bottom)** Permeate from desalination plant.

Table 5. Summary of results for San Juan case study.

Software	Metric	Number of WECs					
		None	1	2	3	4	5
WEC-Sim	Average permeate (m ³ /s)	0	0.0134	0.0245	0.0288	0.0324	0.0348
	Water demand (%)	0.0%	0.9%	1.6%	1.9%	2.2%	2.3%
WNTR	Average pressure (m)	18.4	18.6	18.7	18.8	18.8	18.9
	Average WSA (%)	51%	52%	53%	53%	53%	53%
	Pump power (kW)	0.0	9.9	18.9	22.1	24.7	24.9

4.3. Arecibo Case Study

Arecibo was evaluated for the third case study due to its location on the north shore with a larger wave resource and smaller population. Arecibo has a population of 90,000 people, about twice the size of Guayama and substantially smaller than San Juan [34]. The water demand was scaled assuming the same water consumption rate of 100 gallons per person per day, resulting in a demand of 8.8 million gallons per day (about 33,000 m³/day or 0.39 m³/s). The results from the 24 h simulation based on a full day of NDBC Arecibo (41121) buoy data from 1 January 2022 are shown in Table 6.

The WEC-Sim results show that the wave-powered desalination plant in Arecibo meets 3.8% of the demand for a single WEC farm, 7.0% with two WECs, 8.4% with three WECs, 9.2% with four WECs, and 9.7% of the water demand with a five WEC farm. The permeate and WSA for Arecibo are the highest of the case studies. The average permeate for a single WEC farm was 0.0146 m³/s, 0.0268 m³/s for two WECs, and 0.0375 m³/s for a five WEC farm.

The WNTR results show that the corresponding WSA increased from 54% to 58% for the single and two WEC farms and increased to 60% for the five WEC farms. As with the San Juan case, average water pressure remains low, indicating that the system is compromised and not capable of providing high pressure water for firefighting. Pump power is similar to the other case study sites.

In addition to the 24 h simulation from 1 January 2022, seasonality is also assessed by running the Arecibo cases for 1 April, 1 July, and 1 October 2022. These months correlate to the meteorological seasons as defined by the American Meteorological Society [35]. The seasonality assessment results are shown in Figure 6. The Arecibo seasonality cases were run for a single WEC and five WECs to establish the lower and upper bounds of the analysis. As shown in Figure 3c,d, April is the month with the largest average wave height, and October has the smallest. These months correspond to the largest and smallest average permeate, respectively, for both the single and five WEC farms. Based on this analysis, the maximum permeate of 0.0233 m³/s from the single WEC farm in April 2022 does not exceed the minimum permeate of 0.0271 m³/s from the five WEC farms in October 2022. The effect of the seasonal wave resource on the permeate production and water demand is clear, with the largest permeate and highest percent water demand for both cases occurring in April 2022, the month with the largest wave resource.

Table 6. Summary of results for Arecibo case study.

Software	Metric	Number of WECs					
		None	1	2	3	4	5
WEC-Sim	Average permeate (m ³ /s)	0	0.0146	0.0268	0.0323	0.0355	0.0375
	Water demand (%)	0.0%	3.8%	7.0%	8.4%	9.2%	9.7%
WNTR	Average pressure (m)	20.4	21.2	21.9	22.2	22.2	22.3
	Average WSA (%)	51%	54%	58%	59%	59%	60%
	Pump power (kW)	0.0	11.0	20.9	24.5	24.7	25.0

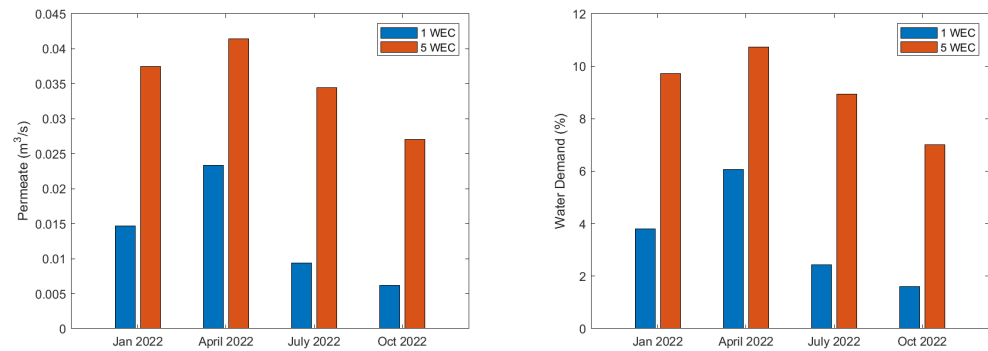


Figure 6. Average permeate and percent water demand delivered by the single WEC and five WEC desalination plants across seasons.

5. Discussion

Integration of a secondary water source into a water distribution system model requires the fine-tuning of modeling constraints. Water distribution systems are designed to distribute treated water from a location where sufficient water supply, pumping, and pipe diameter is available to meet the needs of the surrounding community. The addition of a new water source within that system might not be optimal for the original design of the water distribution system. One challenge of adding water from a desalination plant located on the coast is that the water supply must be pressurized to transport the water to higher elevations in the community. In cases where wave energy is producing a small amount of permeate, the pump can only operate when water storage has reached a critical threshold needed for pumping to ensure the pump has adequate flow. To model a secondary supply of treated water that requires pumping, careful consideration is needed to define the pumping controls.

The case studies suggest that wave-powered desalination is a viable option for producing freshwater in coastal communities. Figure 7a shows the average permeate outputs for all three locations from their respective 24 h simulations. Arecibo has the highest average permeate, and Ponce has the lowest. This is expected because the wave resource off of the south shore is less than that on the north shore, as described in the wave resource section. San Juan has a slightly lower permeate than Arecibo but supplies the lowest percentage of the population's water demand, as seen in Figure 7b. Conversely, Guayama generates the lowest permeate but contributes to the largest percent of the water demand. Trade-offs between these factors should be considered when selecting the location of a wave-powered desalination plant.

While the permeate outputs for Arecibo are the largest, the population is larger and therefore, the percent demand met is lower than in Guayama. Deploying a wave-powered desalination plant on the scale of one to five WECs in San Juan is not the most effective, as the wave resource does not allow for adequate water production for a population of its size. However, the communities of Guayama and Arecibo are less populated and more remote than the capital city of San Juan. Furthermore, the permeate output could be increased in San Juan by designing a larger wave-powered desalination plant.

Figure 7c–e compare the water pressure, WSA, and pump power across all three case studies. The disruption scenario causes average system pressure to decline from a normal operating condition of 60 m to approximately 20 m when the reservoir flow is cut in half. Communities with larger populations, and therefore higher water needs, have a harder time regaining water pressure even with the addition of permeate water. Using higher capacity pumps, or changing the location where the permeate ties into the water distribution system, could improve system pressure. WSA, the fraction of water that people

receive compared to the expected water demand, is reduced to approximately 50% when no permeate is available during the disruption. WSA improvements are related to the increase in permeate from the RO units. Guayama sees the greatest increase, from just over 50% with no desalination to 68% with five ROs. This increase of 18% is directly related to the increase in permeate water demand. Pump power at the desalination plant approaches 25 kW for all three sites as the number of PR units increases from one to five. This is related to the amount of time the pumps are on. Higher permeate fills the desalination tank at a faster rate, allowing the pump to pull water into the water distribution system at a constant rate. From a resilience perspective, the results indicate that desalination can increase WSA even when the water pressure has not returned to normal. This could serve water needs but reduce the ability to use the system for firefighting purposes. As more RO units are used, a continuous power supply is needed to transfer the water into the distribution system.

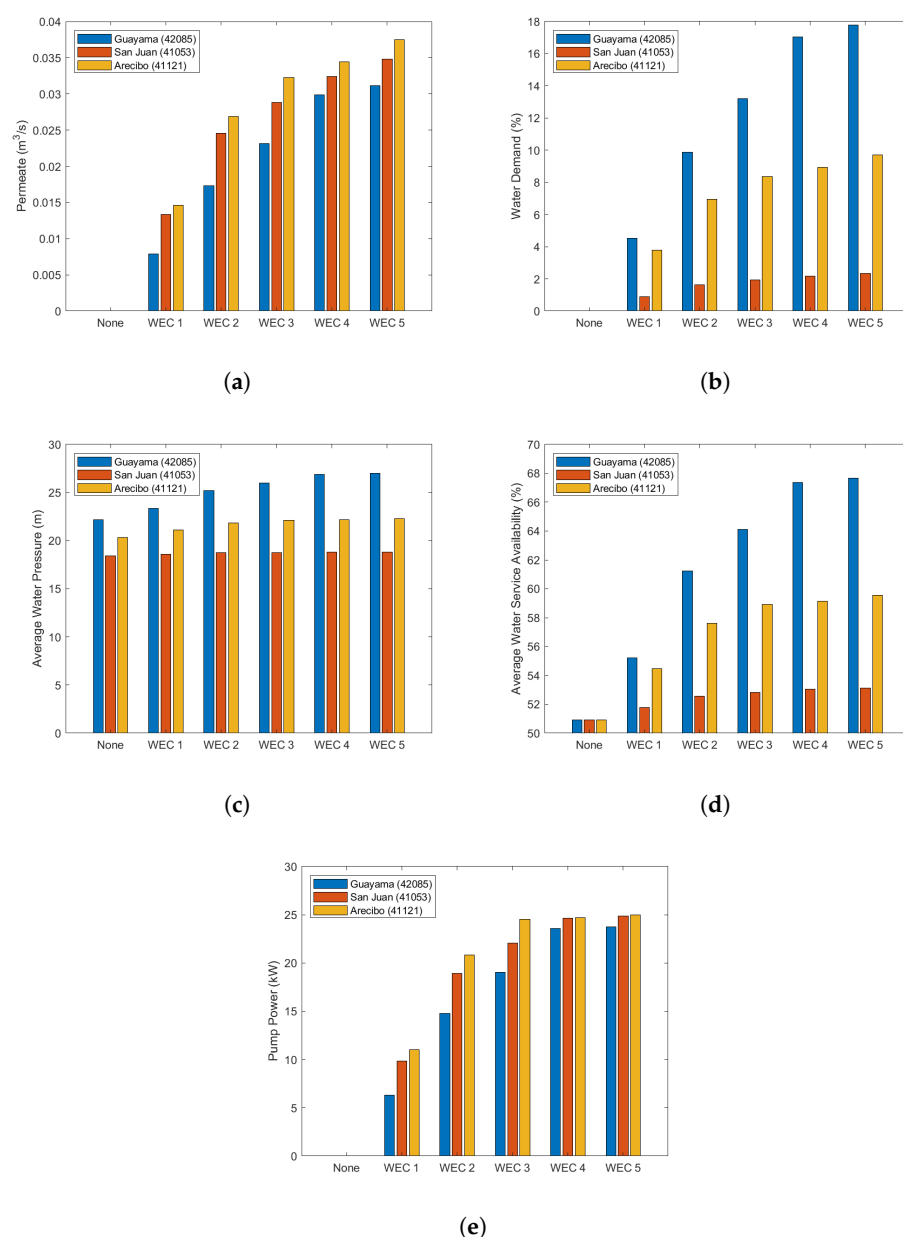


Figure 7. Case study results for Guayama, San Juan, and Arecibo: (a) Permeate. (b) Water demand. (c) Average water pressure. (d) Average water service availability. (e) Pump power.

6. Conclusions

This research integrates expertise across multiple engineering disciplines, including marine energy and drinking water systems. To our knowledge, water distribution system models have not previously been integrated with models of desalination from wave resources. The intersection of these fields requires careful consideration for ensuring both systems are properly represented.

A simulation framework was created by integrating WEC-Sim and WNTR. Resilience metrics were defined to quantify the performance of the coupled software. These metrics were compared using three case studies to determine the impact of wave-powered desalination in producing freshwater and strengthening the resilience of coastal communities. This study applies the simulation framework to three locations in Puerto Rico and discusses trade-offs to be considered when siting a wave-powered desalination plant. Wave-powered desalination is well aligned with both the PBE initiative and, in the case of Puerto Rico, the Puerto Rico Public Policy Act. This strengthens the resilience of island communities by increasing the capacity and self-sufficiency of the utility systems.

Future research will include performing a sensitivity analysis on the case studies to better understand the relationship between resilience metrics and model inputs. Further analysis will also be performed using site-specific water distribution system models, the integration of finer-grained time series in the analysis, and the ability to analyze the co-generation of power and water by the system. Furthermore, the simulation framework can be expanded to group metrics, like water service availability by geographic regions and demographics, to extract additional information on community resilience and vulnerability.

Author Contributions: Conceptualization, K.R. and K.A.K.; methodology, K.R. and K.A.K.; software, K.R. and K.A.K.; formal analysis, K.R., K.A.K. and M.H.; investigation, K.R., K.A.K. and M.H.; data curation, K.R.; writing—original draft preparation, K.R., K.A.K., M.H. and J.G.; writing—review and editing, K.R., K.A.K., M.H. and J.G.; visualization, K.R.; supervision, K.R.; project administration, K.R.; funding acquisition, K.R. and K.A.K. All authors have read and agreed to the published version of the manuscript.

Funding: Funding provided by the U.S. Department of Energy, Office of Energy Efficiency and Renewable Energy, Water Power Technologies Office. Sandia National Laboratories is a multimission laboratory managed and operated by the National Technology & Engineering Solutions of Sandia, LLC, a wholly-owned subsidiary of Honeywell International Inc., for the U.S. Department of Energy's National Nuclear Security Administration under contract DE-NA0003525.

Institutional Review Board Statement: Not applicable.

Informed Consent Statement: Not applicable.

Data Availability Statement: The software used in this study is openly available on GitHub at <https://github.com/WEC-Sim/WEC-Sim> (accessed on 18 December 2024) and <https://github.com/USEPA/WNTR> (accessed on 18 December 2024). The data supporting the conclusions of this article will be made available by the authors on request.

Acknowledgments: This paper describes objective technical results and analysis. Any subjective views or opinions that might be expressed in the paper do not necessarily represent the views of the U.S. Department of Energy or the United States Government.

Conflicts of Interest: The authors declare no conflict of interest.

References

1. LiVecchi, A.; Copping, A.; Jenne, S.; Gorton, A.; Preus, R.; Gill, G.; Robichaud, R.; Green, R.; Geerlofs, S.; Gore, S.; et al. *Powering the Blue Economy: Exploring Opportunities for Marine Renewable Energy in Various Maritime*; Technical Report; National Renewable Energy Laboratory (NREL): Golden, CO, USA, 2019.
2. International Energy Agency. *Net Zero by 2050: A Roadmap for the Global Energy Sector*; Technical Report; IEA: Paris, France, 2021. Available online: <https://www.iea.org/reports/net-zero-by-2050> (accessed on 1 December 2024).
3. Ozkop, E.; Altas, I.H. Control, power and electrical components in wave energy conversion systems: A review of the technologies. *Renew. Sustain. Energy Rev.* **2017**, *67*, 106–115. [\[CrossRef\]](#)
4. Astariz, S.; Iglesias, G. The economics of wave energy: A review. *Renew. Sustain. Energy Rev.* **2015**, *45*, 397–408. [\[CrossRef\]](#)
5. Yu, Y.H.; Jenne, D. Analysis of a Wave-Powered, Reverse-Osmosis System and its Economic Availability in the United States. In *Proceedings of the ASME 2017 36th International Conference on Ocean, Offshore and Arctic Engineering, OMAE 2017*, Trondheim, Norway, 25–30 June 2017; Volume 57786, p. V010T09A032.
6. King, C.W.; Duncan, I.J.; Webber, M. *Water Demand Projections for Power Generation in Texas*; Technical Report; Bureau of Economic Geology, John A. and Katherine G. Jackson School of Geosciences at The University of Texas at Austin: Austin, TX, USA, 2008. Available online: <https://www.twdb.texas.gov> (accessed on 1 December 2024).
7. Bazilian, M.; Rogner, H.; Howells, M.; Hermann, S.; Arent, D.; Gielen, D.; Steduto, P.; Mueller, A.; Komor, P.; Tol, R.S.; et al. Considering the energy, water and food nexus: Towards an integrated modelling approach. *Energy Policy* **2011**, *39*, 7896–7906. [\[CrossRef\]](#)
8. Yu, Y.H.; Jenne, D. Numerical Modeling and Dynamic Analysis of a Wave-Powered Reverse-Osmosis System. *J. Mar. Sci. Eng.* **2018**, *6*, 132. [\[CrossRef\]](#)
9. National Oceanic and Atmospheric Administration. NOAA: Economics and Demographics. 2024. Available online: <https://coast.noaa.gov/states/fast-facts/economics-and-demographics.html> (accessed on 18 December 2024).
10. Ezcurra, P.; Rivera-Collazo, I.C. An assessment of the impacts of climate change on Puerto Rico’s Cultural Heritage with a case study on sea-level rise. *J. Cult. Herit.* **2018**, *32*, 198–209. [\[CrossRef\]](#)
11. Alderson, D.L.; Bunn, B.B.; Eisenberg, D.A.; Howard, A.R.; Nussbaum, D.A.; Templeton, J.I. *Interdependent Infrastructure Resilience in the US Virgin Islands: Preliminary Assessment*; Technical Report; Naval Postgraduate School: Monterey, CA, USA, 2018.
12. Ogden, D.; Ruehl, K.; Yu, Y.H.; Keester, A.; Forbush, D.; Leon, J.; Tom, N. Review of WEC-Sim development and applications. *Int. Mar. Energy J.* **2022**, *5*, 293–303. [\[CrossRef\]](#)
13. Ruehl, K.; Keester, A.; Forbush, D.; Grasberger, J.; Husain, S.; Leon, J.; Ogden, D. WEC-Sim v6.0. 2024. Available online: <https://zenodo.org/records/10023797> (accessed on 1 December 2024).
14. Klise, K.A.; Bynum, M.; Moriarty, D.; Murray, R. A software framework for assessing the resilience of drinking water systems to disasters with an example earthquake case study. *Environ. Model. Softw.* **2017**, *95*, 420–431. [\[CrossRef\]](#) [\[PubMed\]](#)
15. Klise, K.; Moglen, R.; Hogge, J.; Eisenberg, D.; Haxton, T. Resilience analysis of potable water service after power outages in the US Virgin Islands. *J. Water Resour. Plan. Manag.* **2022**, *148*, 05022010. [\[CrossRef\]](#) [\[PubMed\]](#)
16. Chu-Ketterer, L.J.; Murray, R.; Hassett, P.; Kogan, J.; Klise, K.; Haxton, T. Performance and resilience analysis of a New York drinking water system to localized and system-wide emergencies. *J. Water Resour. Plan. Manag.* **2023**, *149*, 05022015. [\[CrossRef\]](#) [\[PubMed\]](#)
17. Coe, R.G.; Yu, Y.H.; Van Rij, J. A survey of WEC reliability, survival and design practices. *Energies* **2017**, *11*, 4. [\[CrossRef\]](#)
18. Silander, M.F.C.; Moreno, C.G.G. On the spatial distribution of the wave energy resource in Puerto Rico and the United States Virgin Islands. *Renew. Energy* **2019**, *136*, 442–451. [\[CrossRef\]](#)
19. Lee, C. *WAMIT Theory Manual*; Massachusetts Institute of Technology: Cambridge, MA, USA, 1995.
20. National Data Buoy Center. Meteorological and Oceanographic Data Collected from the National Data Buoy Center. 2020. Available online: <https://www.ndbc.noaa.gov/> (accessed on 18 December 2024).
21. Governor’s Office of Puerto Rico. GIS Infrastructure Database Puerto Rico. 2015 Available online: <https://gis.pr.gov/descargaGeodatos/Infraestructuras> (accessed on 18 December 2024).
22. WNTR. Water Network Tool for Resilience (WNTR) Website. Available online: <https://usepa.github.io/WNTR> (accessed on 18 December 2024).
23. Flanagan, B.E.; Gregory, E.W.; Hallisey, E.J.; Heitgerd, J.L.; Lewis, B. A social vulnerability index for disaster management. *J. Homel. Secur. Emerg. Manag.* **2011**, *8*, 0000102202154773551792. [\[CrossRef\]](#)
24. Molina, W.L. *Source, Use and Disposition of Freshwater in Puerto Rico, 2010*; Technical Report 2015-3044; US Geological Survey: Reston, VA, USA, 2015.
25. Gómez-Gómez, F.; Rodríguez-Martínez, J.; Santiago, M. *Hydrogeology of Puerto Rico and the Outlying Islands of Vieques, Culebra, and Mona*; Technical Report 3296; US Geological Survey: Reston, VA, USA, 2014.
26. Cantelon, J.A.; Guimond, J.A.; Robinson, C.E.; Michael, H.A.; Kurylyk, B.L. Vertical saltwater intrusion in coastal aquifers driven by episodic flooding: A review. *Water Resour. Res.* **2022**, *58*, e2022WR032614. [\[CrossRef\]](#)

27. Loukas, A.; Vasiliades, L.; Tzabiras, J. Climate change effects on drought severity. *Adv. Geosci.* **2008**, *17*, 23–29. [[CrossRef](#)]
28. USDA Caribbean Climate Hub. Drought Effects on Forests and Rangelands in the US Caribbean. 2016. Available online: <https://www.climatehubs.usda.gov/hubs/caribbean/topic/drought-effects-forests-and-rangelands-us-caribbean> (accessed on 18 December 2024).
29. Torres-González, S.; Rodríguez, J.M. *Hydrologic Conditions in the South Coast Aquifer, Puerto Rico, 2010–15*; Technical Report 2015-1215; US Geological Survey: Reston, VA, USA, 2016.
30. Michener, W.K.; Blood, E.R.; Bildstein, K.L.; Brinson, M.M.; Gardner, L.R. Climate change, hurricanes and tropical storms, and rising sea level in coastal wetlands. *Ecol. Appl.* **1997**, *7*, 770–801. [[CrossRef](#)]
31. Commonwealth of Puerto Rico. *Puerto Rico Energy Public Policy Act*; Act. No. 17 of April 11, 2019; Gobierno de Puerto Rico: San Juan, Puerto Rico, 2019.
32. González-Mejía, A.M.; Ma, X.C. The emergy perspective of sustainable trends in Puerto Rico from 1960 to 2013. *Ecol. Econ.* **2017**, *133*, 11–22. [[CrossRef](#)] [[PubMed](#)]
33. Oki, D.; Gingerich, S.; Whitehead, R. *Ground Water Atlas of the United States: Alaska, Hawaii, Puerto Rico and the US Virgin Islands*; US Geological Survey: Reston, VA, USA, 1999.
34. United States Census Bureau. Puerto Rico: 2020 Census. 2020. Available online: <https://www.census.gov/library/stories/state-by-state/puerto-rico-population-change-between-census-decade.html> (accessed on 18 December 2024).
35. Trenberth, K.E. What are the seasons? *Bull. Am. Meteorol. Soc.* **1983**, *64*, 1276–1282. [[CrossRef](#)]

Disclaimer/Publisher’s Note: The statements, opinions and data contained in all publications are solely those of the individual author(s) and contributor(s) and not of MDPI and/or the editor(s). MDPI and/or the editor(s) disclaim responsibility for any injury to people or property resulting from any ideas, methods, instructions or products referred to in the content.